

# RSC Advances



This is an *Accepted Manuscript*, which has been through the Royal Society of Chemistry peer review process and has been accepted for publication.

*Accepted Manuscripts* are published online shortly after acceptance, before technical editing, formatting and proof reading. Using this free service, authors can make their results available to the community, in citable form, before we publish the edited article. This *Accepted Manuscript* will be replaced by the edited, formatted and paginated article as soon as this is available.

You can find more information about *Accepted Manuscripts* in the [Information for Authors](#).

Please note that technical editing may introduce minor changes to the text and/or graphics, which may alter content. The journal's standard [Terms & Conditions](#) and the [Ethical guidelines](#) still apply. In no event shall the Royal Society of Chemistry be held responsible for any errors or omissions in this *Accepted Manuscript* or any consequences arising from the use of any information it contains.

Cite this: DOI: 10.1039/c0xx00000x

www.rsc.org/xxxxxx

ARTICLE TYPE

## Fabrication of Molds for PDMS Microfluidic Devices by Laser Swelling of PMMA

Ednan Joanni,<sup>\*a</sup> Jonnas Peressinotto,<sup>a</sup> Patricia Silva Domingues,<sup>a,b</sup> Grazielle de Oliveira Setti<sup>a,b</sup> and Dosil Pereira de Jesus<sup>b</sup>

<sup>5</sup> Received (in XXX, XXX) XthXXXXXXXXXX 20XX, Accepted Xth XXXXXXXXXXXX 20XX

DOI: 10.1039/b000000x

The process of volume increase experienced by Polymethylmethacrylate (PMMA), a common thermoplastic material, when subjected to a fast heating-cooling cycle by the action of an ultraviolet laser beam has been investigated in this work. The effects of laser power, focusing, writing speed, cooling and number of exposures on the dimensions of ridges formed by surface swelling were quantified. The biggest swellings, having near Gaussian cross-sectional shapes, were obtained by performing the laser treatments with the polymer immersed in water. The laser swelling technique was applied to the fabrication of molds for microfluidic chips made from Polydimethylsiloxane (PDMS) and the results of the study are discussed within this framework. The method allows the rapid fabrication of molds having a very smooth finish, providing dimensional accuracy appropriate for replication of complex PDMS microfluidic devices.

### Introduction

Microfluidic devices are the subject of intense research due to the possibility of achieving the miniaturization of the entire laboratory setup where chemical reactions and analyses of chemical and biological processes are normally performed.<sup>1,2</sup> The inherent advantages of this concept, currently termed “lab-on-a-chip”, are analogous to the ones brought about by the increasing functionality and cost reduction taking place in the field of microelectronics.<sup>2,3</sup>

The most widely used material for building microfluidic chips is PDMS and the standard procedure for obtaining the molds for polymer casting and device construction is photolithography on silicon, directly borrowed from developments in the micro-fabrication of silicon electronic devices.<sup>4-6</sup> In spite of its obvious advantages, this is a time-consuming process, requiring a clean-room environment and the fabrication of masks, which decrease the degree of flexibility for testing new chip designs.<sup>7,8</sup> With the intention of speeding up the whole process of design and manufacture, and for simplifying the testing of new microfluidic configurations, several authors have proposed alternative methods for mold fabrication, frequently supporting their arguments on cost-saving considerations.<sup>4,5,8-11</sup>

Direct writing of microfluidic channels (by ablation) using lasers is a good approach towards fast and flexible processing. Several types of lasers have been used for this purpose and the range of materials employed is remarkable. However, direct laser writing is not a process free of problems, especially when the applications intended for the microfluidic device require very smooth channel walls. Laser ablation tends to generate a rough surface finish and other problems like edge swelling, re-

deposition of debris, width fluctuations, bubbles or micro-cracking, depending on the material being removed, on the wavelength of the laser, pulse repetition rate, pulse duration and other processing parameters.<sup>7,12-16</sup> Furthermore, the procedure of PDMS casting using a reusable mold allows the fast replication of devices, thus decreasing their individual cost.

Laser polymer swelling has great potential as a technique for mold fabrication, since the surface finish of the original part tends to be unaffected by the interaction with the laser, because the process occurs in the bulk of the material, not on its surface.<sup>17-19</sup> The phenomenon was first described decades ago, but the magnitude of the reported increase in volume was minimal, with typical values of “bump” formation less than a micron in height.<sup>20,21</sup> In spite of an earlier controversy regarding the physical mechanism behind the swelling phenomenon,<sup>17,20,22-25</sup> the melting and subsequent fast cooling of the laser-treated region leading to an amorphous, lower density polymer structure should be responsible for the observed volume increase, according to Li and co-workers.<sup>19</sup> These authors have recently reported the fabrication of microfluidic channel molds in polystyrene using a CO<sub>2</sub> laser.

In this work, using an ultraviolet laser, a study of the effects of laser power, writing speed, focusing, number of scans and cooling method on the surface swelling of PMMA was carried out. This direct-writing laser technique was applied to the fabrication of molds for microfluidic chips made from PDMS.

### Experimental Procedure

All the experiments were executed on clear PMMA sheets 4mm thick. The system for laser micro-fabrication is formed by a

frequency-tripled Nd:YVO<sub>4</sub> pulsed UV laser working at the 355 nm wavelength (Spectra Physics, Pulseo 355-20) and computer-controlled (Newport XPS-C8 motion controller) translation stages in a three orthogonal axis configuration (Newport IMS400-  
5 LM for X and Y and Newport VP-5ZA for Z axis). The laser beam having a Gaussian intensity distribution ( $M^2 < 1.3$ ) was focused on the PMMA using a 50 mm focal length plano-convex lens. The smallest spot size achievable with the existing optical configuration is around 20  $\mu\text{m}$ . The image in Figure 1 shows a  
10 schematic drawing of the laser treatment setup. It should be noticed that the treatments were applied through sample translation under a stationary laser beam, and not by beam steering over a static sample. This arrangement allows for greater precision at the cost of writing speed.

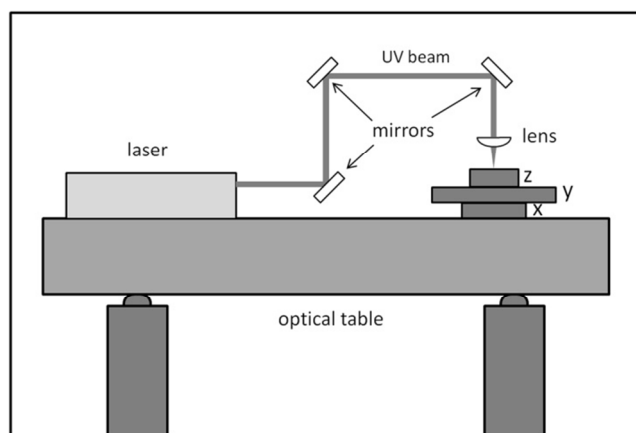


**Fig. 1** Schematic drawing showing the main components and the configuration of the laser-processing system used in this work.

Laser treatments were applied to the PMMA sheets using a combination of parameters. The conditions were chosen in a way  
20 that allowed us to study the effects of the laser on the width and height of swollen lines generated on the PMMA surface. Laser power, translation speed (laser scanning speed), focusing (laser spot size), number of laser scans and cooling rate (natural cooling, nitrogen jet, water immersion) were the processing  
25 variables selected. The applied laser power was in the range between 0.1 W and 1 W, the translation speed between 0.5 mm/s and 5 mm/s, the spot size varied between 20  $\mu\text{m}$  and 200  $\mu\text{m}$  (by changing “Z” and, therefore, the lens-sample distance) and the number of laser sweeps (when more than one sweep was  
30 performed) was up to 4.

The effects of the main parameters of laser treatment on the swelling of PMMA surfaces were studied by optical (Nikon SMZ745) and scanning electron microscopy (FEI, Inspect F50). The samples were covered by a thin sputtered layer of gold in  
35 order to increase their electrical conductivity for the scanning electron microscope (SEM) observations. The surface profile and roughness of the swollen regions was assessed with a stylus profilometer (Bruker, Dektak XT). The same equipment was used for profiling PDMS channels made from the fabricated PMMA  
40 molds.

In order to illustrate the suitability of the method in a real application, a microfluidic PDMS device was built using a PMMA mold obtained by the laser-swelling process. The device included four straight channels (approximately 40  $\mu\text{m}$  deep and

45 400  $\mu\text{m}$  wide cross-section) and was sealed with a glass having regions which included gold-covered oxide nanostructures, such that the nanostructured surfaces were placed inside the microchannels. The nanostructured regions were used as intensifiers for Raman signals by the surface enhanced Raman  
50 scattering (SERS) effect, a strategy to increase the signal by several orders of magnitude.<sup>26</sup> Detection of crystal violet at very low concentrations (up to  $10^{-6}$  molar) by surface-enhanced Raman scattering was performed on aqueous solutions inside the microchannels using a spectrometer Raman Station 400 F (Perkin  
55 Elmer). The laser was focused at the nanostructured surface and the dye solutions were injected in the microchannels. The spectra were obtained during 80 s in the 200 to 2000  $\text{cm}^{-1}$  range. The peak height at 1171  $\text{cm}^{-1}$ , relative to the ring breathing mode, was used for evaluation and comparison of the results.

## 60 Results and Discussion

The role of the main process variables was determined through a series of experiments performed always with the PMMA plates immersed in distilled water (see next sub-section). In this way, the effects of changes in the laser power, writing speed  
65 (translation speed) and laser focusing (spot size) on the dimensions and shape of the surface profiles of the laser-treated regions were assessed. The incremental increase in swelling obtained after successive laser exposures (laser passes) at the same surface regions was also quantified. The other conditions  
70 for the experiments were fixed at arbitrary values in order to isolate the effects of individual variables. The height and width (at the base) of the Gaussian-like profiles were plotted as a function of each of the parameters under study.

### Effect of Cooling

75 The heat transfer rate on the workpiece surface during laser treatment had a striking effect on the profile of ridges formed on the PMMA surface. When no forced cooling was supplied, the maximum bump height achieved was around 10  $\mu\text{m}$ . Any attempt to raise this height by increasing the laser power or by decreasing  
80 the scanning speed caused the cross-sectional profile of the ridges to become highly irregular, deviating from the smooth near-Gaussian shape normally obtained. By directing a high speed jet of nitrogen gas to the region illuminated by the laser, an improvement in the maximum ridge height could be achieved but,  
85 once again, higher bump profiles led to a deformation of the desired regular, symmetric shape. Figure 2 shows examples of irregular surface profiles resulting from the laser treatments when the sample was subjected to natural cooling or to forced cooling by a high speed gas stream.

90 Confirming the results obtained by Li and co-workers,<sup>19</sup> when the sample was allowed to cool naturally, the height of the swollen lines was directly proportional to the laser power, as long as the volume of material heated by the laser treatment was small. The same behaviour could be observed when the samples were  
95 cooled by flowing nitrogen. For higher laser fluences (energy densities per unit area of sample surface) the relaxation of the heat-expanded, low viscosity PMMA under its own weight led to the deformed (non-Gaussian) profiles observed after sample cooling.

100 The range of ridge heights and widths that could be fabricated

was significantly enlarged by immersing the PMMA pieces in water (at 23°C) for the laser treatments. The higher heat exchange rate provided by the liquid in contact with the laser-treated regions was the key to achieving bigger permanent swells.

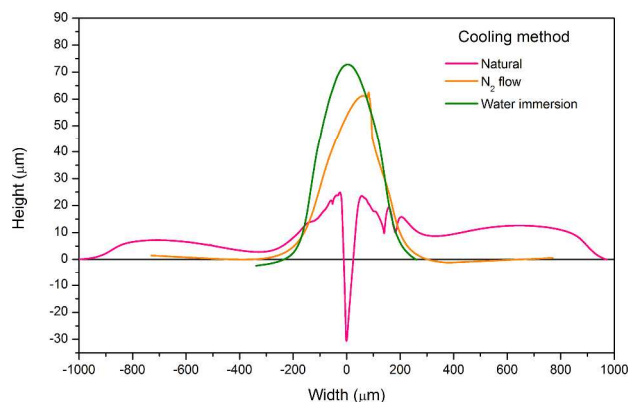


**Fig. 2** Cross-sectional profiles of swollen ridges formed on the surface of PMMA upon laser treatments performed under different cooling methods.

The faster cooling stabilized the volume increase due to laser treatment, preventing the affected region from relaxing back towards the original surface height. In order to keep constant the amount of refraction acting on the laser beam, the distance between the water surface and the PMMA was fixed at 3 mm. Figure 2 shows an example of ridge shape resulting from a laser-writing experiment performed under water. One can notice that the near-Gaussian cross-sectional profile of the ridge is very smooth and the height is bigger than the ones achieved by the other cooling methods. In all three cases, the laser power used was 0.5 W and the sample was translated at 1 mm/s in relation to the laser spot on the polymer surface.

### Effect of UV Exposure

The increase in laser power corresponded to an increase in the width and height of the swollen ridges formed on the surface, as expected. The changes in both dimensions followed the same trend across the whole range of laser powers studied, as shown in Figure 3. For powers above 600 mW one can notice an increase

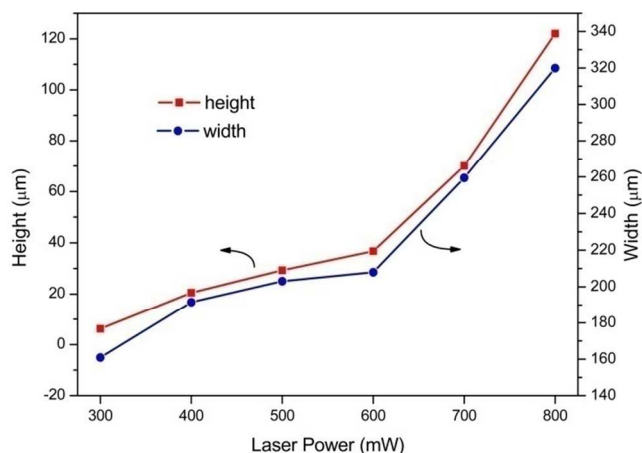


**Fig. 3** Effect of laser power on the dimensions of the Gaussian profile cross-sections of swollen ridges on PMMA. The other parameters used in these experiments were:  $Z = -1$  mm,  $V = 4$  mm/s.

in the rate of swelling as a function of laser power, and this increase corresponds to the onset of bubble formation. Above this power level, laser-induced heating and photo-dissociation not only increases the local temperature above the glass transition temperature ( $T_g$ ) of PMMA, but also begins to break the covalent bonds in the polymer chains, forming low molecular weight products in the gas state.<sup>27,28</sup> This threshold for bubble formation depends also on the writing speed, since the effect of laser exposure on the material is always a result of a train of laser pulses acting on a given volume of material for a given period of time. Figure 4 shows optical microscopy images, taken in cross section, of two ridges where a large number of these laser-generated bubbles is clearly visible.

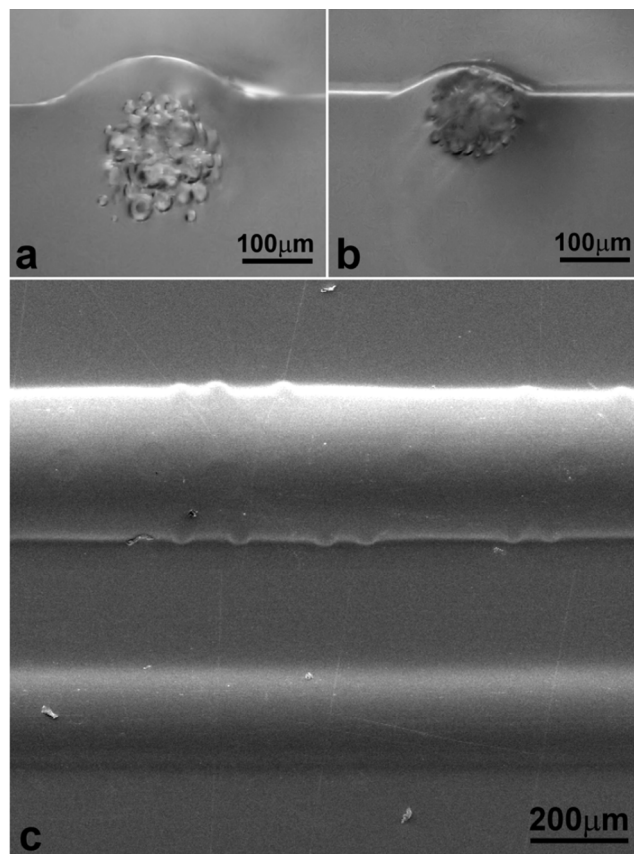


**Fig. 4** Cross section images of gas bubbles inside surface bumps generated in a PMMA plate by a combination of high laser power and low writing speed. a) bubbles in the bulk and b) reaching the sample surface. c) SEM image of laser-swollen tracks on PMMA showing the presence of bubbles appearing at the surface of the top track, where a lower writing speed was used. The lower ridge, made at a higher writing speed, is very smooth.

As long as the bubbles do not reach the surface (see Fig. 4a), their formation do not necessarily mean the cross-sectional profiles are ruined. The profile distortion (with the concurrent increase in surface roughness) only happens when the UV dosage (a combination of time and intensity) is high enough to decrease the polymer viscosity beyond a point where the bubbles are able to reach the surface (Fig. 4b). This argument is further illustrated by the scanning electron microscope image, shown in Figure 4c, of two ridges grown on PMMA using different laser writing speeds. In both cases the exposed regions had bubbles, whose

presence was inferred through visual inspection and confirmed by optical microscopy observation. Contrary to the optical microscope, the SEM shows only the surface relief of the samples. The circular depressions and protuberances in the ridge shown in the upper part of the image are a consequence of bubbles appearing at the sample surface, in a clear contrast to the smooth surface of the ridge on the lower part of the image, written using a higher translation speed.

The use of high laser power levels focused close to the sample surface ( $Z$  values around zero) generates fluence values high enough to be above the material ablation threshold. Figure 5 shows an optical microscope photograph of a ridge with a central dark line where the PMMA was ablated. The image was taken with reflected light, so the debris of ejected material re-deposited on the sample surface could be easily noticed. The ablation takes place only at the center of the ridge because the Gaussian laser beam energy profile exhibits the highest intensity at the center of the laser spot.

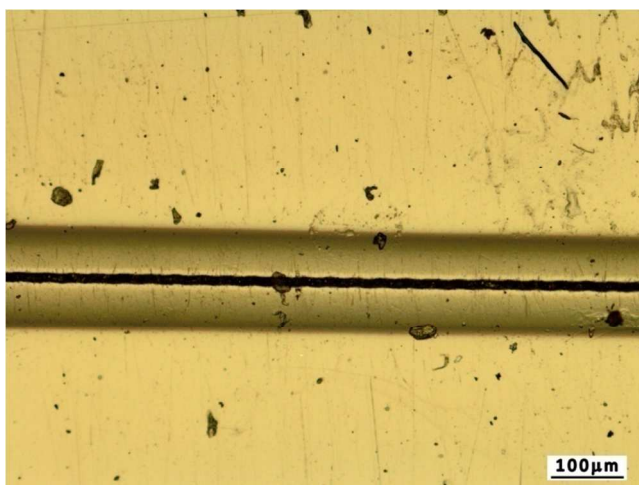


**Fig. 5** Reflected light optical image of a high power laser-generated ridge on PMMA showing an ablated trench at the center line.

The translation speed of the material in relation to the laser beam had an effect on the dimensions of the swollen regions that mirrored the one from laser power. In this case, decreases in translation speed corresponded to increases in the surface bumps produced, as seen in the graph of Figure 6. Once again, the change in the slope of the curves below 3 mm/s marks the onset of bubble formation, and is related to an increase in laser dosage, as previously discussed.

The effects of cumulative exposures of PMMA regions to the laser are illustrated by the results shown in Figure 7. After the first laser treatment, which created a ridge with a cross-sectional profile having a 17  $\mu\text{m}$  height, the next exposure of the same region increased the initial height by 33%, the next one by 10%, and the fourth by 7.5%, indicating that there is a tendency to reach a stable ridge height after enough number of treatments. On the other hand, the width of the near-Gaussian profile was practically unaffected by the number of laser passes, since the first and the fourth exposures resulted in ridges with profiles having widths of 187  $\mu\text{m}$  and 191  $\mu\text{m}$ , respectively. The increase in ridge heights with cumulative exposures is more pronounced when the combination of processing conditions is such that the initial swelling is relatively small. This can be explained, once

again, taking into consideration the notion that the swelling effect is a product of a “laser dose” (a combination of the effects of laser power and exposure time). If a combination of high laser power, low translation speed and focusing near the sample surface are used, the initial swelling is large and subsequent exposures have little further effect on these regions.

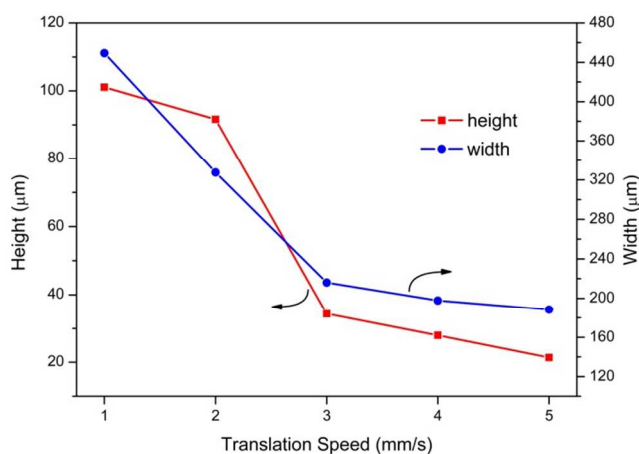


**Fig. 6** Effect of translation speed on the dimensions of the Gaussian profile cross-sections of swollen ridges on PMMA. The other parameters used in these experiments were:  $Z = -1$  mm,  $P = 0.5$  W.

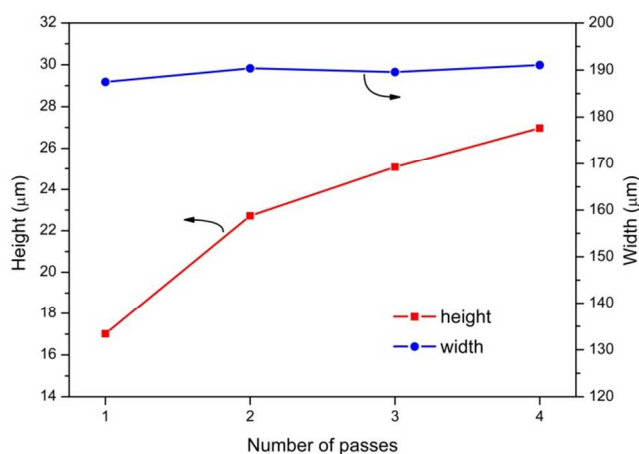


**Fig. 7** Effect of the number of passes on the dimensions of the Gaussian profile cross-sections of swollen ridges on PMMA. The parameters used were:  $Z = -1$  mm,  $V = 4$  mm/s,  $P = 0.4$  W.

#### Effect of Position of Focal Plane

The effect of laser focusing on the ridge profiles is shown in Figure 8. In this case, the height and width of the near-Gaussian shapes are affected by the focusing in almost exactly the opposite way. When the laser is focused on the polymer surface ( $Z = 0$ ), the illuminated spot size is the smallest possible (around 20  $\mu\text{m}$  diameter). The heating effect from laser exposure is concentrated near the PMMA surface and the temperature gradient across the XY plane tends to be steep due to the relatively low thermal conductivity of the polymer and the water cooling. As a consequence, the height of the swelling is large and the width tends to be small. As the values of  $Z$  increase, the sample is brought closer to the lens, putting the focal point inside the material. As a consequence, the fluence on the surface decreases, the spot size gets larger and the heated region expands and gets buried below the surface. This accounts for the gradual decrease

in bump height and the simultaneous increase in width. The sample movement in the opposite direction ( $Z = -1$ ) puts the focal point above the surface and the beam is diverging when it reaches the PMMA. This tends to concentrate the heating effect near the sample surface even more than before, but the effect on the surface profile of the swollen region was not so pronounced in this case.

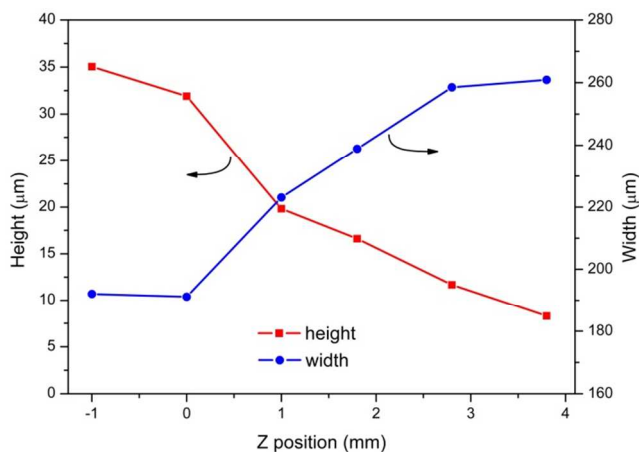


**Fig. 8** Effect of focus position on the dimensions of the Gaussian profile cross-sections of swollen ridges on PMMA. The other parameters used in these experiments were:  $V = 4$  mm/s,  $P = 0.5$  W. Negative values are above the surface and positive values are inside the material.

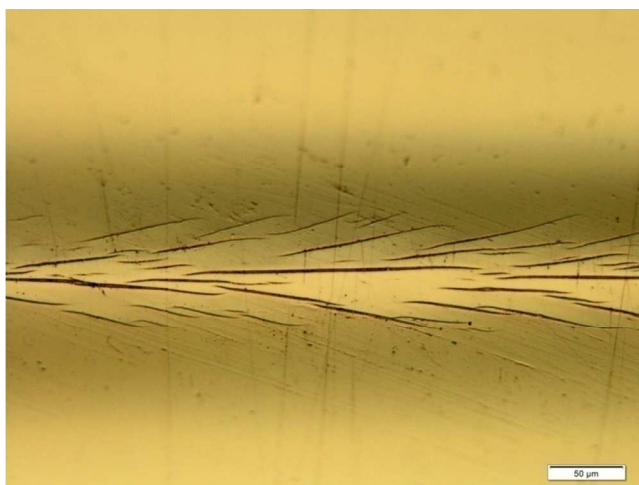


**Fig. 9** Shallow surface cracking observed when a combination of high translation speed and deep laser focusing was used.

A peculiar kind of defect observed in some samples used in these experiments is shown in Figure 9. This surface cracking appeared only when a very specific set of processing parameters was employed. When the laser was focused deep below the surface and high translation speeds were used, shallow surface cracks (around  $1 \mu\text{m}$  depth) remained on the sample surface as the beam was swept from left to right in the photograph. The source of these defects could be explained as follows: The laser pulse energy remains constant as  $Z$  approaches the focal point, so the intensity increases strongly along with the decrease in the beam cross section. At the laser head exit, the beam is  $3.6$  mm in diameter, while at the focal point the diameter drops to approximately  $20 \mu\text{m}$ . In our case, having a beam diameter of  $3.6$  mm,  $5$  cm focal length lens and laser pulse energy of  $200 \mu\text{J}$ , the

energy density at the sample surface (known as Fluence,  $F$ ) can be calculated according to Equation 1 as:

$$F(\text{mJ}/\text{cm}^2) = \frac{0.2}{\pi(0.036|z|)^2} \quad (1)$$

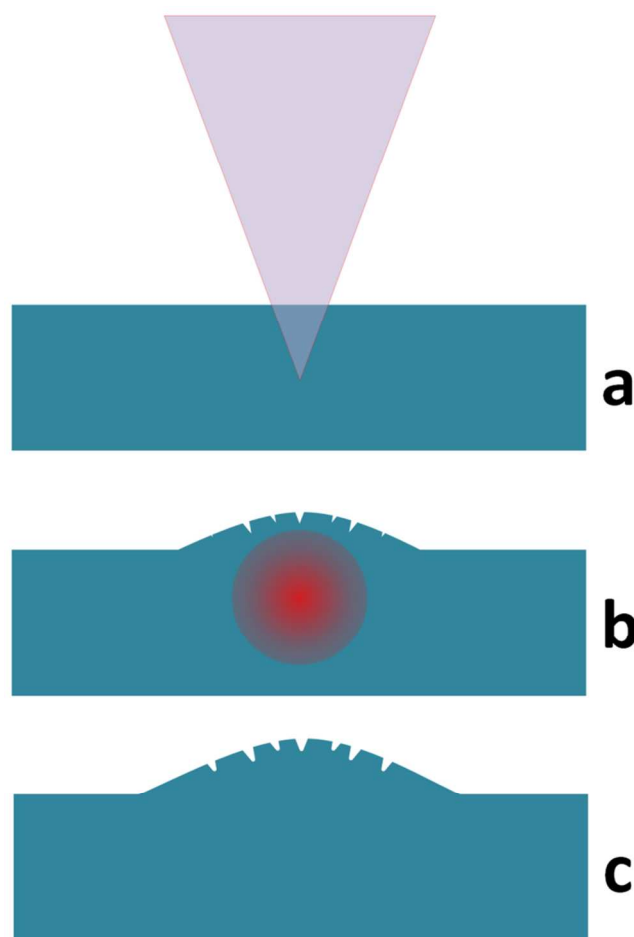


**Fig. 10** Schematic representation of the process responsible for surface cracking: a) the laser is focused deep inside the material; b) the heated polymer expands, putting the surface under traction and nucleating cracks; c) after the sample cools down to room temperature the polymer remains with a cracked ridge.

When the laser beam is focused on the sample surface, the fluence is  $6.4 \times 10^4 \text{ mJ}/\text{cm}^2$ . On the other hand, when the focus is shifted  $2$  mm inside the sample, the fluence on the surface decreases to  $1.3 \times 10^3 \text{ mJ}/\text{cm}^2$ . This drop in fluence of more than one order of magnitude is enough to create the sequence of events illustrated schematically in Figure 10: Upon reaching the sample (Figure 10a) the laser beam has its diameter decreased until the pulse heats a volume of material near the focal point located a few millimeters under the surface. The localized heating causes an increase in volume (Figure 10b), but the region near the surface has a lower temperature due to the lower fluence and the cooling effect from the water. After laser exposure, the sample cools down to room temperature and part of the swelling remains, along with a number of surface cracks due to the expansion of surface material happening at a temperature below the  $T_g$  of PMMA (Figure 10c). This kind of defect could be easily eliminated by shifting the focus to a position closer to the surface

or by decreasing the translation speed. These two operations, either alone or combined, allowed the surface temperature of the sample to increase, reaching values above the  $T_g$  of PMMA (around 110°C).

### 5 Surface Quality and Reproducibility

The reproducibility of the ridges obtained by laser processing was tested by building a mold for a microfluidic device having four channels, generating the PDMS device and by performing cross-sectional profile measurements on the resulting PDMS channels.

The results of these measurements, performed at eight locations chosen at random, are shown in Figure 11.

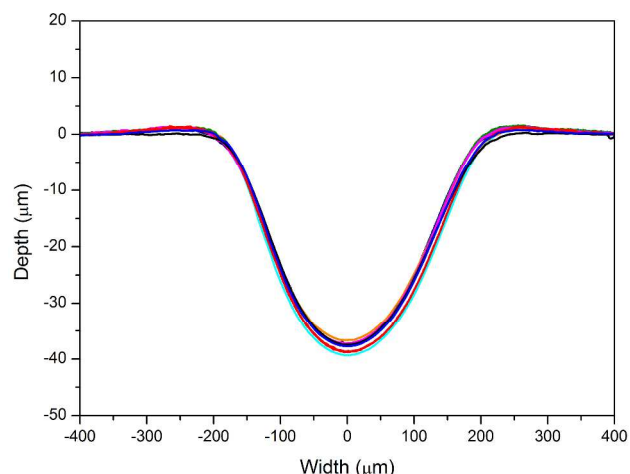


**Fig. 11** Cross-sectional profiles of PDMS channels taken at eight points chosen at random.

The spread in the dimensions of the microfluidic channels is relatively small. Under the processing conditions used, the average depth of the channels is 37.8 μm and the standard deviation 0.855, with the largest deviation being only 4.1% of the average depth. For the channel widths, the reproducibility was even better, with an average of 373 μm, a standard deviation of 5.01 and the biggest discrepancy being only 2.1% of the average width. The average roughness ( $R_a$ ) of the laser-treated areas of the mold, measured on four random positions was 6.4 nm, being very similar to the original value of 4.1 nm measured on the pristine PMMA plate.

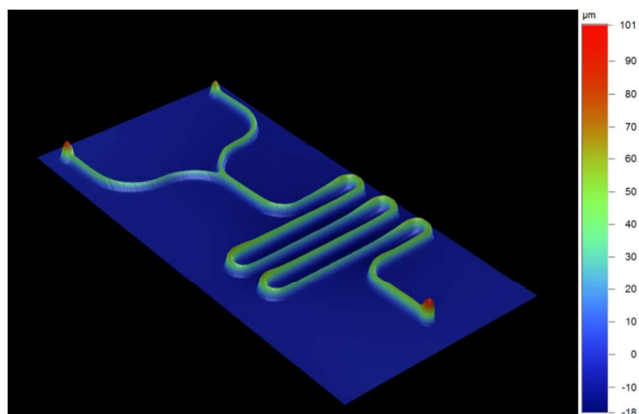


**Fig. 12** Surface map of a PMMA mold for a PDMS microfluidic device obtained by the laser swelling method.

The color-coded surface map of a PMMA mold for a microfluidic device shown in Figure 12 illustrates the quality of the surface finish afforded by the direct laser writing method described in this work. This microfluidic device mold was obtained from a drawing in less than five minutes.

### Testing of Fabricated PDMS Devices

Figure 13 shows the spectra obtained with the crystal violet solutions. This molecule exhibits a very low signal/noise ratio and it is clear that the device worked very well in the intensification of the peak of interest at 1171  $\text{cm}^{-1}$ . The higher concentration reached peak intensity higher than  $1 \times 10^5$ , allowing easy detection of the analyte. Even for the lowest concentration, 1 μM, the signal exceeded  $1 \times 10^3$ , and it was still possible to detect the crystal violet. These results show that the PDMS devices fabricated using the PMMA molds are efficient for use in microfluidic SERS detection.

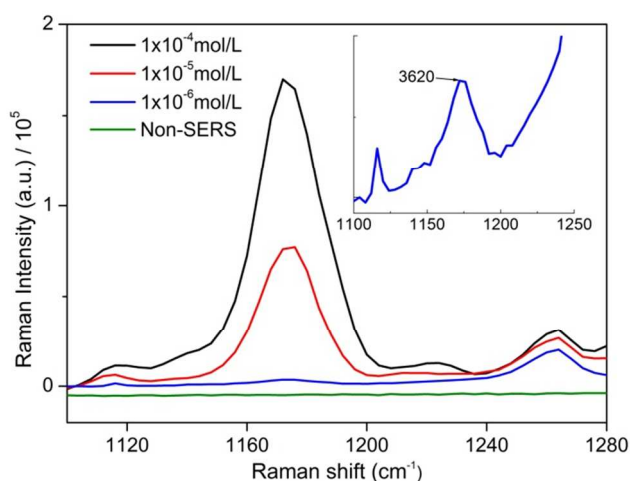


**Fig. 13** Raman spectra obtained using the PDMS/glass microfluidic device for different crystal violet concentrations. The inset is a magnification of the spectrum relative to the  $1 \times 10^{-6}$  mol/L concentration.

### Conclusions

The present mold manufacturing technique for replication of PDMS microfluidic devices displays a set of desirable characteristics which are not easily matched by any single established method. The process is fast, since the molds can be manufactured in a matter of minutes, from design to the finished product. The surface finish of the formed ridges is excellent, because polymer swelling is a bulk phenomenon; therefore, the original surface roughness is kept virtually unchanged in the final parts produced. The method is very flexible and reproducible, allowing the fabrication of microfluidic PDMS devices incorporating channels with different widths and depths, achievable through simple alterations in the processing variables. These characteristics should appeal to researchers and institutions involved in the development and/or fabrication of PDMS microfluidic devices, especially if a laser processing system is already available or if its demand for other applications could help to justify the initial cost.

Apart from highlighting the general trends regarding the effect of selected variables, the limits for the process could also be determined in the experiments reported in this work. The lower

limit appears when a combination of low power, high translation speed and large spot size is used. Under these conditions no polymer swelling is produced. On the other extreme (high laser power, low translation speed and small spot size) defects are generated, either on the surface itself or in the bulk of the sample, due to excessive heating and/or photo-dissociation, leading to bubbles or even to material ablation at higher laser powers.

Performing the fabrication process with the PMMA immersed in water was crucial for reaching faster cooling rates and much higher degrees of surface swelling, thus expanding the range of dimensions for the microfluidic channels produced. The present method should easily be extended to other polymeric materials. Crystalline or partially crystalline thermoplastics should, in principle, provide the biggest differences in volume between laser-treated and untreated regions, therefore generating swollen surface features with bigger dimensions.

### Acknowledgements

We would like to acknowledge the support of the Brazilian Nanotechnology National Laboratory (LNNano) in the SEM work. This work was supported by the National Council of Technological and Scientific Development (CNPq, grant n° 305318/2012-8) and the São Paulo Research Foundation (FAPESP, grants n° 2013/25108-9 and n° 2013/22485-6).

### Notes and References

<sup>a</sup>Centro de Tecnologia da Informação Renato Archer (CTI), Rod. Dom Pedro I km 143.6, 13069-901, Campinas, SP, Brazil. E-mail: ednan.joanni@cti.gov.br  
<sup>b</sup>Instituto de Química, Universidade Estadual de Campinas (Unicamp), Caixa postal 6154, 13083-970, Campinas, SP, Brazil.

1. T. M. Squires and S. R. Quake, *Rev. Mod. Phys.*, 2005, **77**, 977-1026.
2. H. A. Stone, A. D. Stroock and A. Ajdari, *Annu. Rev. FLUID Mech.*, 2004, **36**, 381-411.
3. D. Erickson and D. Q. Li, *Anal. Chim. Acta*, 2004, **507**, 11-26.
4. D. C. Duffy, J. C. McDonald, O. J. A. Schueller and G. M. Whitesides, *Anal. Chem.*, 1998, **70**, 4974-4984.
5. J. C. McDonald and G. M. Whitesides, *Accounts Chem. Res.*, 2002, **35**, 491-499.
6. T. Fujii, *Microelectron. Eng.*, 2002, **61-2**, 907-914.
7. D. Nieto, T. Delgado and M. T. Flores-Arias, *Opt. Laser Eng.*, 2014, **63**, 11-18.
8. I. J. Micheal, A. J. Vidyasagar, K. K. Bokara, N. K. Mekala, A. Asthana and C. M. Rao, *Lab on a Chip*, 2014, **14**, 3695-3699.
9. J. C. McDonald, M. L. Chabinyc, S. J. Metallo, J. R. Anderson, A. D. Stroock and G. M. Whitesides, *Anal. Chem.*, 2002, **74**, 1537-1545.
10. H. Becker and L. E. Locascio, *Talanta*, 2002, **56**, 267-287.
11. H. Becker and C. Gartner, *Electrophoresis*, 2000, **21**, 12-26.
12. C. K. Chung, Y. C. Lin and G. R. Huang, *J. Micromech. Microeng.*, 2005, **15**, 1878-1884.
13. D. Teixidor, F. Orozco, T. Thepsonthi, J. Ciurana, C. A. Rodriguez and T. Oezel, *Int. J. Adv. Manuf. Tech.*, 2013, **67**, 1651-1664.
14. L. Romoli, G. Tantussi and G. Dini, *Opt. Laser Eng.*, 2011, **49**, 419-427.
15. Z. K. Wang, H. Y. Zheng, R. Y. H. Lim, Z. F. Wang and Y. C. Lam, *J. Micromech. Microeng.*, 2011, **21**.

16. D. Teixidor, T. Thepsonthi, J. Ciurana and T. Özel, *J. Manuf. Process.*, 2012, **14**, 435-442.
17. F. Beinhorn, J. Ihlemann, K. Luther and J. Troe, *Appl. Phys. A-Mater.*, 1999, **68**, 709-713.
18. T. Meunier, A. B. Villafranca, R. Bhardwaj and A. Weck, *Opt. Lett.*, 2012, **37**, 4266-4268.
19. H. Li, Y. Fan, D. Conchouso and I. G. Foulds, *J. Micromech. Microeng.*, 2012, **22**.
20. M. Himmelbauer, E. Arenholz, D. Bauerle and K. Schilcher, *Appl. Phys. A-Mater.*, 1996, **63**, 337-339.
21. T. Masubuchi, H. Furutani, H. Fukumura and H. Masuhara, *J. Phys. Chem. B*, 2001, **105**, 2518-2524.
22. A. Y. Malyshev and N. M. Bityurin, *Quantum Electron.*, 2005, **35**, 825-830.
23. N. Bityurin, *Appl. Surf. Sci.*, 2009, **255**, 9851-9855.
24. A. Y. Malyshev, N. A. Agareva, O. A. Mal'shakova and N. M. Bityurin, *J. Opt. Technol.*, 2007, **74**, 641-646.
25. N. M. Bityurin, *Quantum Electron.*, 2010, **40**, 955-965.
26. E. L. Ru and P. Etchegoin, *Principles of surface enhanced Raman spectroscopy and related plasmonic effects*, Elsevier, Amsterdam, 2009.
27. C. Wochowski, M. A. S. Eldin and S. Metev, *Polymer Degradation and Stability*, 2005, **89**, 252-264.
28. E. Rebolgar, G. Bounos, M. Oujja, S. Georgiou and M. Castillejo, *Appl. Surf. Sci.*, 2007, **253**, 7820-7825.